

Synthesis and crystal structure of zirconium tungstate $\text{ZrW}_2\text{O}_7(\text{OH},\text{Cl})_2 \cdot 2\text{H}_2\text{O}$

Mike S. Dadachov^{a*} and Richard M. Lambrecht^b

^aMaterials Division, Australian Nuclear Science and Technology Organisation, PMB 1 Menai NSW 2234, Australia

^bEberhard-Karls-Universität Tübingen Universitätslink PET-Zentrum, 15 Rontgenweg, D-72076 Tübingen, Germany

$\text{ZrW}_2\text{O}_7(\text{OH},\text{Cl})_2 \cdot 2\text{H}_2\text{O}$ has been synthesised by refluxing, followed by hydrothermal crystallisation of amorphous zirconium tungstate gels in 1–8 M HCl. It is known that the amorphous Zr tungstate can be used as a gel-generator for production of the ^{188}Re medical radioisotope. The structure of $\text{ZrW}_2\text{O}_7(\text{OH},\text{Cl})_2 \cdot 2\text{H}_2\text{O}$ has been refined by conventional powder diffractometer data. The compound crystallises in the tetragonal space group $I4_1cd$ (no. 110) with $a = 11.4454(4)$, $c = 12.4851(7)$ Å, $Z = 8$ and $D_c = 3.74$ g cm^{−3}. Rietveld refinement has been carried out from X-ray diffraction data using Co-K α radiation over the angular range 15–105° (2θ) and converged with $R_{wp} = 8.85\%$, $R_p = 6.60\%$. The structure consists of regular ZrO_7 pentagonal bipyramids and distorted WO_6 octahedra, connected in a three-dimensional framework. The terminal hydroxy groups of tungsten polyhedra are statistically substituted by Cl.

Zirconium tungstate and other inorganic matrix gel-generators for production of ^{188}Re have been extensively studied in recent years.^{1–9} They are obtained as amorphous, non-stoichiometric and non-equilibrium basic salts, evidently depending on the conditions of their aging, washing and drying. Most previously reported zirconium molybdate and tungstate compounds are amorphous precipitate gels, probably best regarded as non-equilibrium basic salts of indefinite stoichiometry. Only two compounds in a crystalline form, $\text{ZrMo}_2\text{O}_7(\text{OH})_2 \cdot 2\text{H}_2\text{O}$ ¹⁰ and $\text{ZrW}_2\text{O}_7(\text{OH})_2 \cdot 2\text{H}_2\text{O}$,¹¹ have been described as discrete inorganic compounds.

The crystal structure of $\text{ZrMo}_2\text{O}_7(\text{OH})_2 \cdot 2\text{H}_2\text{O}$ has been solved from single crystal data. However, zirconium tungstate does not crystallise in the form of large single crystals. In this work we report powder Rietveld refinement of the crystal structure of zirconium tungstate, obtained *via* hydrothermal crystallisation of amorphous zirconium tungstate in concentrated hydrochloric acid.

Experimental

Synthesis

Zirconium tungstate was precipitated at room temperature as a white, amorphous gel by adding first 0.5 M $\text{Na}_2\text{WO}_4 \cdot 2\text{H}_2\text{O}$ and then a solution of 0.5 M $\text{ZrOCl}_2 \cdot 8\text{H}_2\text{O}$ in molar ratio $\text{Zr}/\text{W} = 1$ to 100 ml water. The precipitate was separated by filtration under suction, washed with water and air dried. The zirconium tungstate formed (40 g) was placed in a 1 l round-bottomed flask and refluxed with 500 ml of 11.8 M HCl for several hours at 95°C, and the semicrystalline material was washed with water to remove Na and Cl ions. About 3 g of semicrystalline zirconium tungstate and 30 ml of 4 M HCl were then sealed in a Teflon-lined stainless-steel 45 ml Parr autoclave and heated at 170°C for 5 days. After cooling, the solid was collected by filtration, washed with distilled water and dried in air at 110°C. A highly crystalline sample was prepared by this method. Thermogravimetry was performed to verify the water content.

The synthesis of this material by hydrothermal treatment of the initial amorphous gels was not successful, and always resulted in poorly crystalline powder. Crystallisation kinetics of zirconium tungstate *via* refluxing in HCl at 95°C is illustrated in Fig. 1 (diffraction patterns were obtained using Cu-K α radiation).

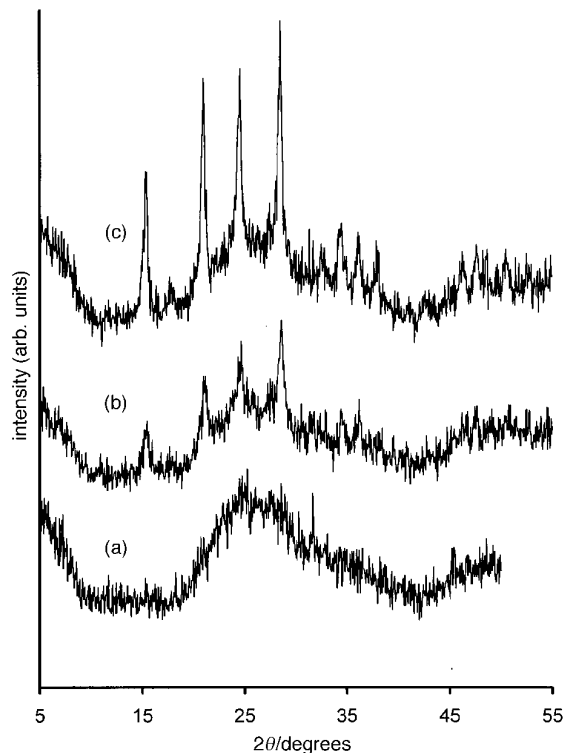


Fig. 1 Crystallisation kinetics of zirconium tungstate (Cu-K α radiation): (a) before treatment, (b) after 4 h treatment, (c) after 8 h treatment

X-Ray diffraction data collection

A D500 Siemens powder diffractometer, using Bragg–Brentano geometry, was used for identification and data collection. The alignment and instrumental resolution of the diffractometer was checked by standard reference materials. Preliminary data from different preparations of the sample revealed a preferred-orientation effect, mainly in direction [001]. A study of the sample by scanning electron microscopy confirmed the later observation, made by X-ray diffraction, and shows that the particles have a platelet morphology with an average size $30 \times 30 \mu\text{m}$. The powder diffraction pattern was scanned in steps of $0.02^\circ(2\theta)$, and a fixed-time count of 10 s. At the end

of the data collection the stability of the incident beam was checked by recording the first lines of the pattern.

Results and Discussion

Rietveld refinement of the structure

The X-ray diffraction pattern was indexed in tetragonal space group $I4_1cd$. Table 1 lists measured and calculated d -spacings with corrected preferred orientation intensities.

Structure refinement, bond-angle calculations and all other calculations were performed by using the Rietveld structure refinement package GSAS.¹² The refinement of the structure of zirconium tungstate was started as usual from a scale factor and three to four terms of background coefficients (Chebyshev

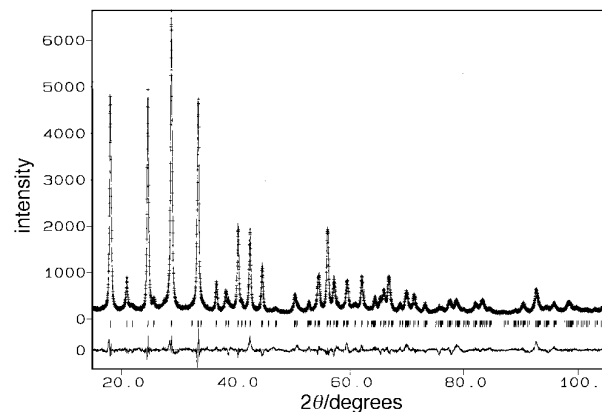


Fig. 2 Observed (+), calculated (solid line) and difference Rietveld plots in the same intensity scale

Table 1 X-Ray powder diffraction data for $\text{ZrW}_2\text{O}_7(\text{OH},\text{Cl})_2 \cdot 2\text{H}_2\text{O}$

hkl	d_{obs}	d_{calc}	I_{obs}^a	I_{calc}^b
200	5.722	5.7227	72	43
112	4.944	4.9430	13	16
211	4.736	4.7360	5	9
202	4.217	4.2184	74	100
220	4.046	4.0466	7	4
310	3.616	3.6194	100	87
312	3.131	3.1311	— ^c	64
004	3.122	3.1213	71	58
400	2.859	2.8614	12	6
204	2.739	2.7402	9	7
402	2.602	2.6011	29	37
420	2.559	2.5593	6	4
332	2.475	2.4764	29	29
314	2.363	2.3637	17	32
431	2.250	2.2446	4	2
404	2.109	2.1092	8	4
116	2.015	2.0153	6	4
206	1.955	1.9556	15	17
600	1.907	1.9076	29	28
532	1.871	1.8725	13	16
316	1.804	1.8040	13	13
541	1.796	1.7694	5	2
622	1.738	1.7381	14	15
406	1.683	1.6829	7	11
534	1.662	1.6616	7	11
336	1.648	1.6477	10	12
604	1.627	1.6277	14	26
640	1.587	1.5872	5	2
008	1.560	1.5606	9	6
642	1.538	1.5382	8	12
730	1.503	1.5029	5	4
800	1.431	1.4307	6	6 ^d

^aPreferred orientation [001]. ^bCorrected intensities from Rietveld refinement results. ^cOverlap. ^dOwing to similar unit-cell parameters and a high degree of peak overlap high hkl values are not listed.

polynomials of the first type) using initial atomic positional parameters, described in ref. 10 fixed at one isotropic displacement factor for all atoms and derived from powder diffraction pattern unit-cell parameters. Neutral atomic scattering factors were used for all atoms.

The refinement proceeded satisfactorily, and the profile and atomic parameters were added to the model as variables as the refinement progressed. A simple Gaussian model was found to be inadequate to describe the observed peak shape, and a significantly better fit was obtained by using a pseudo-Voigt (Gaussian–Lorentzian) model.¹³ The optimal and stable profile coefficients for the pseudo-Voigt functions were found. Correction for peak asymmetry with simultaneous inclusion of additional background coefficients and preferred orientation [001], by a March–Dollase function,¹⁴ yielded stable overall parameters during all refinement stages.

The initially calculated coordinates of Zr and W were refined with the help of least-squares cycles followed by the refinement of the coordinates of all other atoms. The suitability of the initial model was put in doubt by the mismatch between calculated and observed profiles, viewed during the application of different refinement strategies.

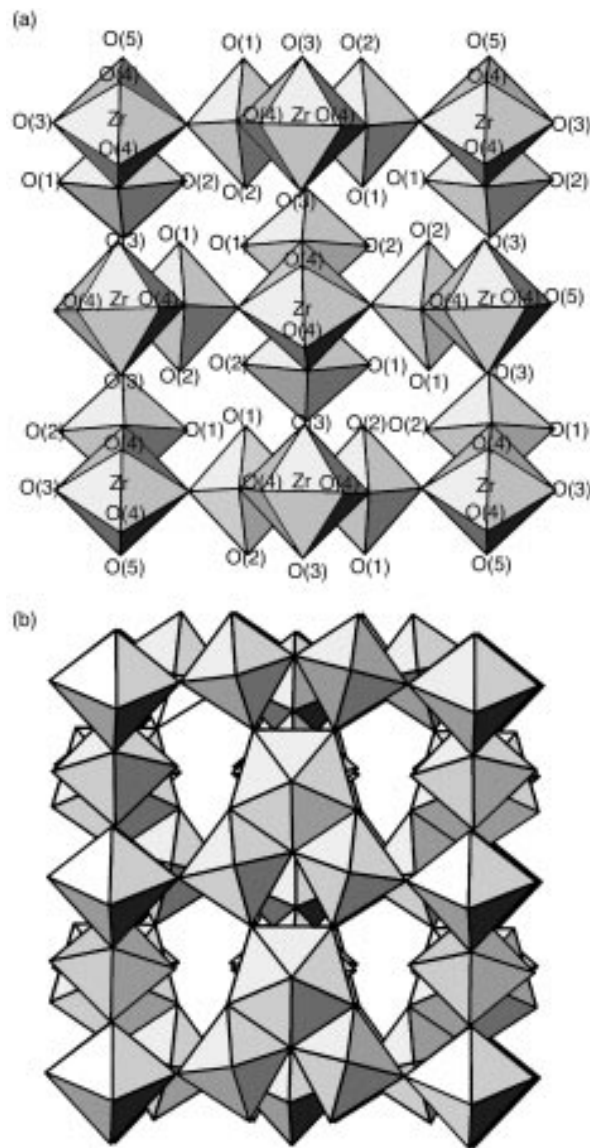


Fig. 3 Polyhedral structure of $\text{ZrW}_2\text{O}_7(\text{OH},\text{Cl})_2 \cdot 2\text{H}_2\text{O}$ viewed down the c (a) and b (b) axes

Those doubts were confirmed by the unstable x coordinate of W atoms. The starting value ($x=0.02471$) of the x coordinate of W was refined to be very close to zero and fluctuated between positive and negative values during the refinement procedure. In the course of the resolution, it was decided to fix the x coordinate of the tungsten atom at $x=0.0$, since it was refined very close to this ideal value (variation between 0.016 and -0.018), but with a large standard deviation (0.01). These fluctuations did not affect the very stable y and z coordinates of tungsten. The mismatch between calculated and observed profiles was particularly noticeable for the intensity of the peak (312).

The solution of this structural problem was found when the energy dispersive microanalysis of our sample, previously exhaustively washed with water, demonstrated the presence of Cl atoms in the sample. Thus, the strongest peaks from a difference-Fourier map can be attributed to the Cl atoms in position $x=0.183$, $y=0.165$, $z=0.247$. Interestingly, in the structure of zirconium molybdate the same position is exclusively occupied by the oxygen of the hydroxy group,¹⁰ whereas as described here, this position in zirconium tungstate is partially occupied by Cl.

The formula of the compound was established as $\text{ZrW}_2\text{O}_7(\text{OH},\text{Cl})_2 \cdot 2\text{H}_2\text{O}$. The final Rietveld refinement plot (observed, calculated and difference profiles) of $\text{ZrW}_2\text{O}_7(\text{OH},\text{Cl})_2 \cdot 2\text{H}_2\text{O}$ are shown in Fig. 2.

Description of structure

Crystallographic data are given in Table 2, final atomic positional and thermal data in Table 3 and bond lengths and angles in Table 4. The crystal structure of $\text{ZrW}_2\text{O}_7(\text{OH},\text{Cl})_2 \cdot 2\text{H}_2\text{O}$ is illustrated in Fig. 3(a) and (b). The

Table 2 Crystallographic and Rietveld refinement data for $\text{ZrW}_2\text{O}_7(\text{OH},\text{Cl})_2 \cdot 2\text{H}_2\text{O}$

molecular formula	$\text{ZrW}_2\text{O}_7(\text{OH},\text{Cl})_2 \cdot 2\text{H}_2\text{O}$
rel. mass of unit cell	3672.75
λ (Co-K α)/ \AA	1.79026
scan range, 2θ /degrees	15–105
step scan increment, 2θ /degrees	0.02
step scan time/s	10
crystal system	tetragonal
space group	14_1cd
$a/\text{\AA}$	11.4454(4)
$b/\text{\AA}$	11.4454(4)
$c/\text{\AA}$	12.4851(7)
Z	8
$D_c/\text{g cm}^{-3}$	3.7428
$V/\text{\AA}^3$	1635.51(8)
$\text{W}–\text{O}$ (av.)/ \AA	2.005
$\text{Zr}–\text{O}$ (av.)/ \AA	2.148
refined profile parameters	26
refined structural parameters	16
$R(F^2)$	7.72
$R_{\text{wp}}(\%)$	8.85
$R_{\text{p}}(\%)$	6.60
reduced χ^2	2.72

Table 4 Selected interatomic distances (\AA) and angles ($^\circ$) for $\text{ZrW}_2\text{O}_7(\text{OH},\text{Cl})_2 \cdot 2\text{H}_2\text{O}$

W–O(1)	1.961(19)	Zr–O(3)	2.144(18)
W–O(2)	2.050(24)	Zr–O(3)	2.144(18)
W–O(3)	1.798(23)	Zr–O(4)	2.094(19)
W–O(3)	1.789(26)	Zr–O(4)	2.094(19)
W–O(4)	2.369(28)	Zr–O(5)	2.200(18)
W–O(5)	2.075(12)	Zr–O(5)	2.200(18)
O(4)–O(6)	1.807(30)	Zr–O(6)	2.220(15)
O(1)–W–O(2)	173.0(4)	O(3)–Zr–O(3)	173.0(5)
O(1)–W–O(3)	106.1(14)	O(3)–Zr–O(4)	93.9(20)
O(1)–W–O(5)	100.0(4)	O(3)–Zr–O(4)	90.5(18)
O(1)–W–O(6)	93.8(19)	O(3)–Zr–O(5)	83.3(11)
O(2)–W–O(3)	74.7(15)	O(3)–Zr–O(5)	94.2(14)
O(2)–W–O(5)	86.6(17)	O(3)–Zr–O(6)	93.4(23)
O(2)–W–O(6)	88.9(13)	O(4)–Zr–O(4)	98.9(19)
O(3)–W–O(5)	93.0(26)	O(4)–Zr–O(5)	62.5(9)
O(3)–W–O(6)	145.4(20)	O(4)–Zr–O(5)	159.7(16)
O(3)–W–O(6)	55.2(11)	O(4)–Zr–O(6)	49.4(9)
W–O(3)–Zr	154.2(17)	O(5)–Zr–O(5)	137.1(18)
W–O(6)–W	130.3(15)	O(5)–Zr–O(6)	111.5(9)
W–O(6)–O(4)	114.9(6)	O(5)–Zr–O(6)	111.5(9)
W–O(6)–O(4)	114.9(13)		

three-dimensional framework Zr and W atoms are located in fully occupied 8a (0,0,z) and 16b (0,y,z) positions; zirconium atoms are found in ZrO_7 pentagonal bipyramids and tungsten atoms are found in WO_6 octahedra.

There is no significant variation of the Zr–O distance within the zirconium coordination sphere (2.09–2.22), which is nearly equal to the sum of the ionic radii of Zr^{4+} and O^{2-} , ($R_{\text{Zr}}^{4+} + R_{\text{O}}^{2-} = 0.80 + 1.40 = 2.2 \text{ \AA}$). The mean Zr–O distance is 2.16 \AA . The slight distortion of Zr polyhedra is caused by sharing its O(5)–O(6) and O(5)–O(8) edges with tungsten octahedra. The Zr is slightly displaced towards opposite edges from the ideal centre of the polyhedra. The O(4) atom is shared between Zr and W in such a way that it is actually the closest of all O atoms to Zr (Zr–O 2.094 \AA) and the furthest from W (W–O 2.369 \AA).

The W–O distances lie in the range 1.79–2.37 \AA , with a mean value of 2.007 \AA and are in good agreement with bond lengths observed in zirconium molybdate, an analogue of this compound containing distorted molybdenum octahedra.⁶ The significantly distorted WO_6 octahedra show three short and three long distances. Such distortion for highly charged small cations has been observed in many previously reported structures.^{15–17} This off-centre disposition of tungsten can be explained by non-equal sharing of the oxygens: long distances for shared and short for terminal oxygens, the central atom being too small to fill the octahedral hole in a van der Waals-packed oxygen octahedron. The bond length W–O(3) (1.789 \AA) is more characteristic for tetrahedrally rather than for octahedrally coordinated W.

The water hydrogens are assigned to O(2) atoms while the

Table 3 Atomic coordinates and isotropic thermal parameters (\AA^2) for $\text{ZrW}_2\text{O}_7(\text{OH},\text{Cl})_2 \cdot 2\text{H}_2\text{O}$

atom	Wyckoff notation	x	y	z	$B_{\text{iso}}/\text{\AA}^2$
W	16b	0.0000(18)	0.16391(17)	0.2389(16)	2.5(2)
Zr	8a	0	0	0	0.8(1)
O(1)	16b	0.1829(19)	0.165(6)	0.249(11)	1.5(2)
Cl(1)	16b	0.1829(19)	0.165(6)	0.249(11)	—
O(2)	16b	–0.1625(21)	0.166(6)	0.237(10)	1.2(13)
O(3)	16b	0.1679(32)	–0.0198(19)	0.001(5)	0.8(1)
O(4)	16b	0.0134(32)	0.1306(21)	–0.1254(31)	0.8(1)
O(5)	16b	0.0299(26)	0.1836(28)	0.0511(30)	0.8(2)
O(6)	8a	0	0	0.193(4)	1(3)

OH and Cl ions are distributed in random fashion over the same O(4) position. Thus, polyhedra have the following formulae: $\text{ZrO}_3\text{O}_2\text{Cl}_2$ for Zr pentagonal bipyramids and $\text{cis}-\text{WO}_4(\text{OH},\text{Cl})(\text{H}_2\text{O})$ for tungsten octahedra. This assignment is in accord with the IR spectrum of zirconium tungstate in which bands characteristic of hydroxy groups (sharp and strong peak at 3345 cm^{-1} , O—H stretching) and aqua groups (broad and strong peak at 3325 cm^{-1} , aqua O—H stretching; 1645 cm^{-1} , aqua O—H bending) are observed.

Conclusions

The solution of the structure of zirconium tungstate helps to explain the chemistry of the ^{188}W — ^{188}Re gel-generator system. The radioactive decay of $^{188}\text{W}^{\text{VI}}$ atoms, which are located in significantly distorted octahedra, results in the formation of radioactive $^{188}\text{Re}^{\text{VII}}$. Rhenium(vii)-188 atoms are located in distorted octahedra but their valency is higher and radius is smaller than $^{188}\text{W}^{\text{VI}}$ (0.56 and 0.65 \AA for $^{188}\text{Re}^{\text{VII}}$ and $^{188}\text{W}^{\text{VI}}$, respectively). This combination of a higher charge and smaller radius results in very loose fitting of $^{188}\text{Re}^{\text{VII}}$ within the highly distorted octahedra and, consequently, in easy washing out of ^{188}Re using slightly polar solvents.

The chemical implication of the zirconium tungstate structure is quite significant. Zirconium tungstate doped with ^{188}W is a matrix for production of the short-lived beta-emitter ^{188}Re which is an important medical radioisotope for cancer therapy. Knowledge of the crystal structure of zirconium tungstate, the only crystalline compound derived directly from a ^{188}W — ^{188}Re gel-generator system, is an important contribution to an understanding of the fundamental chemistry of this gel-generator system.

References

- 1 N. B. Mikheev, V. B. Popovich, I. A. Rumer, G. I. Savelev and N. C. Volkova, *Isotopenpraxis*, 1972, **8**, 248.
- 2 A. P. Gallahan, D. E. Rice and F. F. Knapp, *Nucl. Compact*, 1989, **20**, 3.
- 3 G. Kodina, T. Tulskaya, E. Gureev, G. Brodskaya, O. Gapurova and B. Drosdovsky, in *Technetium and Rhenium in Chemistry and Nuclear Medicine*, 3, ed. M. Nicolini, G. Bandoli and U. Mazzi 1990, p. 635.
- 4 A. P. Gallahan, D. E. Rice, D. W. McPherson, S. Mirzadeh and F. F. Knapp, *Appl. Radiat. Isot.*, 1992, **43**, 802.
- 5 V. O. Kordyukevich and N. P. Rudenko, *Radiokhimya*, 1984, **26**, 625.
- 6 G. J. Ehrhardt, A. R. Ketting, T. A. Tuprin, M-S. Razavi, J-L. E. Vanderheyden, F. M. Su and A. R. Fritzberg, in *Technetium and Rhenium in Chemistry and Nuclear Medicine*, 3, ed. M. Nicolini, G. Bandoli and U. Mazzi, 1990, p. 631.
- 7 J-L. Vanderheyden, F-M. Su and G. J. Ehrhardt, *US Pat.*, 5, 145, 636 Sept. 8, 1992, Int Cl⁵ G 21 G 1/00, US Cl 376/189.
- 8 M. Dadachov, R. M. Lambrecht and E. Hetherington, *J. Radioanal. Nucl. Chem. Lett.*, 1994, **188**, 267.
- 9 M. Dadachov and R. M. Lambrecht, *J. Radioanal. Nucl. Chem. Lett.*, 1995, **200**, 211.
- 10 A. Clearfield and R. H. Blessing, *J. Inorg. Nucl. Chem.*, 1972, **34**, 2643.
- 11 A. Clearfield and R. H. Blessing, *J. Inorg. Nucl. Chem.*, 1974, **36**, 1174.
- 12 A. C. Larson and R. B. Von Dreele, *GSAS User Guide*, Los Alamos National Laboratory, Los Alamos, NM, 1996.
- 13 C. J. Howard, *J. Appl. Crystallogr.*, 1982, **15**, 615.
- 14 W. A. Dollase, *J. Appl. Crystallogr.*, 1986, **19**, 267.
- 15 J. Donohue, *Inorg. Chem.*, 1965, **4**, 921.
- 16 H. D. Megaw, *Acta Crystallogr., Sect. B*, 1968, **24**, 153.
- 17 D. L. Kepert, *Inorg. Chem.*, 1969, **8**, 1556.

Paper 7/01565H; Received 5th March, 1997